Received: 14 October 2021 | Revised: 9 June 2022 | Accepted: 14 June 2022

DOI: 10.1111/mmi.14954

RESEARCH ARTICLE

WILEY

Ino80 is required for H2A.Z eviction from hypha-specific promoters and hyphal development of *Candida albicans*

Qun Zhao[1] | Baodi Dai[1] | Hongyu Wu[1] | Wencheng Zhu[1,2] | Jiangye Chen[1]

[1]State Key Laboratory of Molecular Biology, Shanghai Institute of Biochemistry and Cell Biology, Center for Excellence in Molecular Cell Science, University of Chinese Academy of Sciences, Chinese Academy of Sciences, Shanghai, China

[2]Institute of Neuroscience, CAS Center for Excellence in Brain Science and Intelligence Technology, Chinese Academy of Sciences, Shanghai, China

Correspondence
Wencheng Zhu, Institute of Neuroscience, CAS Center for Excellence in Brain Science and Intelligence Technology, Chinese Academy of Sciences, Shanghai, China.
Email: wczhu@ion.ac.cn

Jiangye Chen, State Key Laboratory of Molecular Biology, Shanghai Institute of Biochemistry and Cell Biology, Center for Excellence in Molecular Cell Science, University of Chinese Academy of Sciences, Chinese Academy of Sciences, Shanghai, China.
Email: jychen@sibcb.ac.cn

Funding information
National Natural Science Foundation of China, Grant/Award Number: 31970144 and 32170196

Abstract

ATP-dependent chromatin remodeling complexes play important roles in many essential cellular processes, including transcription regulation, DNA replication, and repair. Evicting H2A.Z, a variant of histone H2A, from the promoter of hypha-specific genes is required for hyphal formation in *Candida albicans*. However, the mechanism that regulates H2A.Z removal during hyphal formation remains unknown. In this study, we demonstrated that Ino80, the core catalytic subunit of the INO80 complex, was recruited to hypha-specific promoters during hyphal induction in Arp8 dependent manner and facilitated the removal of H2A.Z. Deleting *INO80* or mutating the ATPase site of Ino80 impairs the expression of hypha-specific genes (HSGs) and hyphal development. In addition, we showed that Ino80 was essential for the virulence of *C. albicans* during systemic infections in mice. Interestingly, Arp5, an INO80 complex-specific component, acts in concert with Ino80 during DNA damage responses but is dispensable for hyphal induction. Our findings clarified that Ino80 was critical for hyphal development, DNA damage response, and pathogenesis in *C. albicans*.

KEYWORDS
Arp5, Arp8, *Candida albicans*, H2A.Z removal, Ino80

1 | INTRODUCTION

The commensal fungal species *Candida albicans* is an opportunistic pathogen that causes both superficial and invasive infections in immunocompromised and immunosuppressed patients (Gow et al., 2012; Romani et al., 2003). A characteristic feature of *C. albicans* is its ability to grow in different cellular forms, such as unicellular budding yeast, filamentous pseudohyphae, and true hyphae (Sudbery, 2011; Whiteway & Bachewich, 2007). The morphological transition between yeast and hyphae is critical for *C. albicans* virulence (Dalle et al., 2010).

The dynamic accessibility of the genome is key to the regulation of gene expression. In eukaryotes, these dynamics are ultimately gated by nucleosomes, the fundamental units of chromatin (Clapier et al., 2017). Nucleosomes wrap 147 bp of DNA around an octameric core containing two copies of the highly conserved H3, H4, H2A, and H2B histone proteins (Kornberg & Lorch, 1999; Luger et al., 1997). Placement of nucleosomes at specific positions in the genome can

This is an open access article under the terms of the Creative Commons Attribution-NonCommercial-NoDerivs License, which permits use and distribution in any medium, provided the original work is properly cited, the use is non-commercial and no modifications or adaptations are made.
© 2022 The Authors. *Molecular Microbiology* published by John Wiley & Sons Ltd.

regulate gene function by altering the accessibility of transcription factor-binding sites and facilitating the formation of higher-order chromatin structures (Wyrick et al., 1999). Multi-protein-composed ATP-dependent nucleosome-remodeling complexes use the energy of ATP hydrolysis to specifically disrupt the interactions between histones, thereby achieving chromatin alternation, such as nucleosome sliding, eviction, and reconfiguration (Becker & Horz, 2002). Based on sequence similarities within the common Snf2-type ATPase motor domain, remodelers are generally classified into four families: INO80, SWI/SNF, ISWI, and CHD (Smith & Peterson, 2005).

The INO80 remodeler is an evolutionarily conserved chromatin remodeler that binds nucleosome-free regions around the promoter and transcriptional start sites (TSS) and changes chromatin architecture via nucleosome repositioning (Chakraborty & Magnuson, 2022; Poli et al., 2017). INO80 plays a critical role in many processes, such as DNA damage response, replication, and mitotic stability (Cao et al., 2015; Klopf et al., 2017; Poli et al., 2017). In *Saccharomyces cerevisiae*, the INO80 complex consists of a core ATPase enzyme, Ino80, and 14 other subunits, including Arp5, Arp8, Arp4, Nhp10, Rvb1, Rvb2, and Ies2 (Eustermann et al., 2018; Shen et al., 2000). The yeast Ino80 was first identified in a genetic screen to identify mutants that affect inositol biosynthesis (Ebbert et al., 1999) and structural studies have indicated that Ino80 functions as an assembly scaffold. The species-specific 'Nhp10 module' (Ies1, Ies3, Ies5, and Nhp10) interacts with the N-terminal domain of Ino80; the highly conserved 'Arp8 module' (N-actin, Arp4, Arp8, Ies4, and Taf14) associates with the middle region of Ino80 containing the HSA domain and N-terminal region (Szerlong et al., 2008; Tosi et al., 2013). The Nhp10 and Arp8 modules work synergistically by binding the linker DNA at the nucleosome entry site, which is allosterically coupled to the processive nucleosome translocation catalyzed by INO80 (Yao et al., 2016). The long insertion snf2-type ATPase motor is located at the C-terminus of Ino80, which is critical for the assembly of the Rvb1/Rvb2 helicase and is responsible for the recruitment of Arp5/Ies5 (Jonsson et al., 2004; Zhang et al., 2019). Arp5 and Arp8 are specific to the INO80 complex, which is essential for recruitment and ATPase activity of the INO80 complex. Deleting each of these two genes results in a phenotype similar to that of the *ino80* deletion mutant in the DNA damage response (Drengk et al., 2004; Takahashi et al., 2017; Zhao et al., 2010).

Removal of H2A.Z from chromatin near the damage sites, which is achieved by the INO80 complex, is required for homologous recombination (Alatwi & Downs, 2015). H2A.Z is a canonical histone variant that participates in many processes such as transcriptional regulation, gene silencing, and genome stability (Lademann et al., 2017; Subramanian et al., 2015). In *C. albicans*, SWR1 complex-mediated incorporation of H2A.Z into nucleosomes near hypha-specific promoters or opaque-specific promoters is required for the maintenance of the yeast state (Wang et al., 2018) or white state (Guan & Liu, 2015). During hyphal induction, H2A.Z is rapidly evicted from hypha-specific promoters (Wang et al., 2018). However, the mechanism underlying H2A.Z removal during hyphal induction remains unknown. In this study, we demonstrated that Ino80, which is the core catalytic subunit of the INO80 complex in *C. albicans* and contributes to the virulence of *C. albicans* during systemic infections, is recruited to the promoter regions of hypha-specific genes (HSGs) and mediates H2A.Z eviction, further activating the expression of HSGs and promoting hyphal development.

2 | RESULTS

2.1 | *C. albicans* Ino80 plays an important role in hyphae formation

The INO80 complex, an evolutionarily conserved ATP-dependent chromatin remodeler, is involved in gene regulation and DNA damage response through the removal of H2A.Z from promoters and for maintenance of genome integrity (Lademann et al., 2017; Poli et al., 2017). Since H2A.Z was rapidly evicted from hypha-specific promoters during hyphal induction in *C. albicans* (Wang et al., 2018), we wondered whether it was mediated by a conserved INO80 complex. First, we analyzed the *C. albicans* database and found a predicted Ino80 in the *C. albicans* genome (http://www.candidagenome.org/). Sequence comparison revealed that the predicted *C. albicans* Ino80 (*Ca*Ino80) was highly conserved with its counterparts from *S. cerevisiae* Ino80 (*Sc*Ino80) and *H. sapiens* Ino80 (*Hs*Ino80). All of these contain an N-terminal helicase/SANT-associated (HSA) domain and a C-terminal ATPase domain, which contains a variable large insertion (Figure 1a). To investigate the functional roles of Ino80 in H2A.Z eviction and hyphae formation, we deleted both copies of *CaINO80* from the *C. albicans* genome and constructed an *ino80* null mutant strain. Unlike wild-type (Bailey et al., 2004) cells, *ino80* mutant cells were defective in hyphal induction, with delayed hyphal initiation and shortened hyphal elongation under hyphal growth conditions (37°C, YPD containing 10% serum) (Figure 1b,c). The *swr1* mutant cells formed long hyphae under the same conditions, which was in line with previous findings (Wang et al., 2018). Deletion of the H2A.Z encoding gene (*HTZ1*) shared a phenotype similar to that of the *swr1* mutant. The deficiency of the *ino80* mutant in hyphal development was more obvious when cultured in YPD without serum, and all *ino80* mutant cells formed yeast-like cells, whereas the *htz1* and *swr1* mutant cells formed true hyphae under the same growth conditions (Figure 1b,c), suggesting that Ino80 has an opposite role to Swr1 in hyphal induction. Defects in hyphal filament formation associated with *ino80* mutants have also been observed in solid medium. On serum-containing agar medium, the wild-type strain generated florid hyphal colonies, whereas the *ino80* mutant formed short filamentous colonies (Figure 1d). On solid Lee's medium, the *ino80* mutant failed to develop filamentous colonies, whereas the wild-type colonies were surrounded by long filaments (Figure 1d). On a solid YPD plate, the wild-type strain formed long filaments beneath the surface, whereas the *ino80* mutant formed short, thinner filaments (Figure 1e). Thus, Ino80 is required for filamentous and invasive growth.

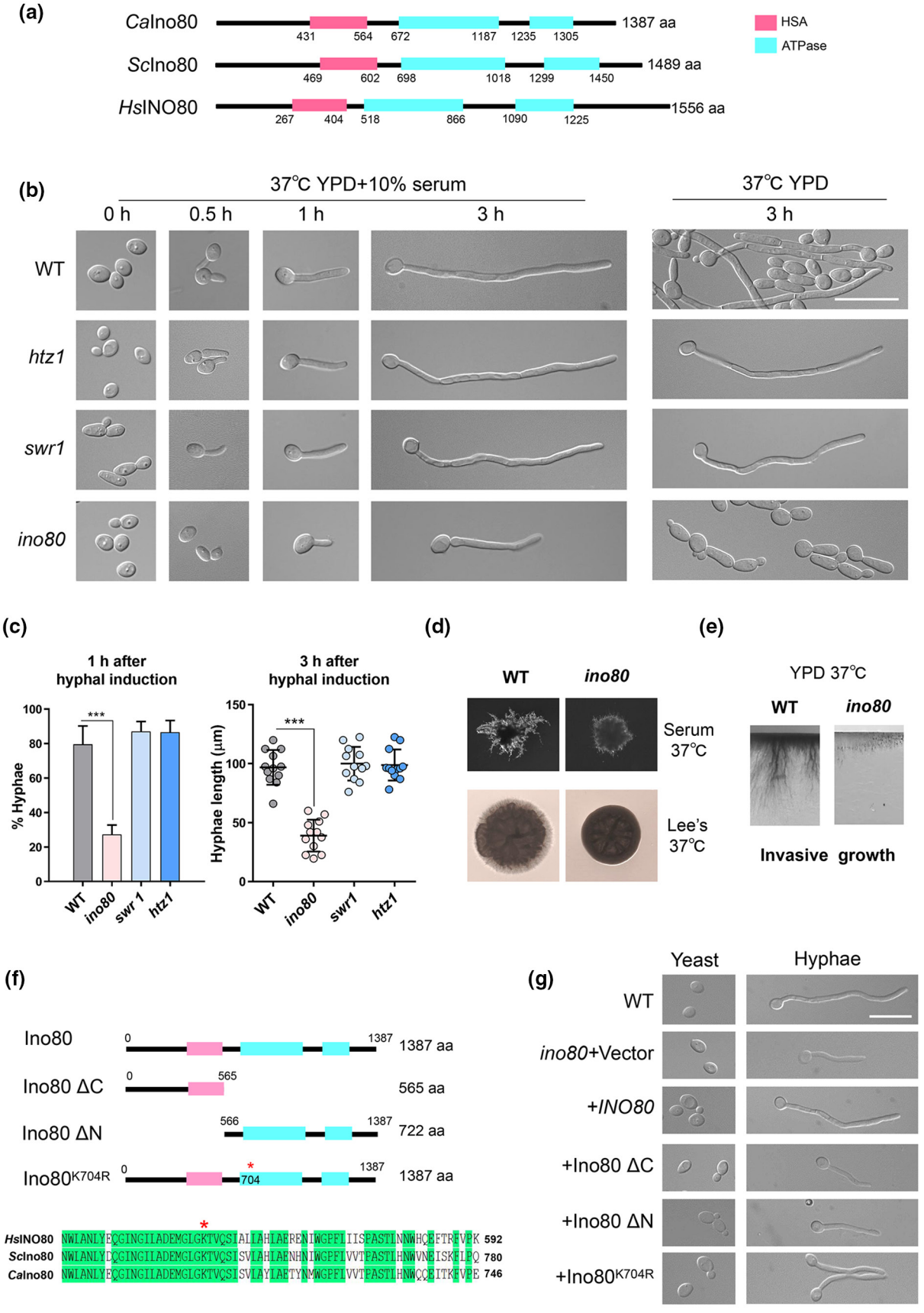

To analyze the effects of the Ino80 domains on hyphae formation, we introduced ectopically expressed wild-type Ino80 and Ino80 mutants into the *ADE2* locus under the control of the *ADH1* promoter. The wild-type Ino80 revertant could fully restore hyphal formation (Figure 1f,g), whereas the two truncation mutants lacking the C-terminus and N-terminus could not rescue the true hyphae

formation of the *ino80* mutant strain (Figure 1f,g). The lysine residue at 704 of *Ca*Ino80 is a predicted ATPase activity site conserved from yeast to humans and is required for the ATPase activity of Ino80 in yeast (Ebbert et al., 1999). When lysine was replaced with alanine, the Ino80^{K704A} mutant failed to recover in the hyphal development (Figure 1f). To verify that the revertant strains could fully express the truncated or full-length *INO80*, we designed domain-specific primers and measured their expression by qRT-PCR (Figure S1a). It is shown that the wild-type *INO80* and *INO80* mutants were efficiently expressed in all the revertant strains (Figure S1b). We further constructed the HA-tagged proteins to confirm the stability of wild-type Ino80 and Ino80 mutant proteins. Western blot analysis showed that the ectopically expressed Ino80 and Ino80 mutant proteins are stable (Figure S1c). Taken together, we demonstrated that *C. albicans* Ino80 was required for hyphal formation and that ATPase activity was essential for Ino80 function.

2.2 | Recruiting of Ino80 to hypha-specific promoters for upregulating the expression of hypha-specific genes

A previous report suggested that Ino80 was recruited to chromatin to regulate gene expression (Wang et al., 2014). To explore whether Ino80 acts in a similar manner in *C. albicans*, we performed chromatin immunoprecipitation (ChIP) followed by quantitative real-time polymerase chain reaction (qRT-PCR) to determine the occupancy of Ino80 at the promoter regions of HSGs using primers targeting the promoter regions of *ECE1*, *HWP1*, and *ALS3* (Table S3). A Myc tag was fused to the C-terminus of Ino80 under the control of its own promoter, and the results showed that the abundance of Ino80 associated with HSG promoters was dynamically regulated during hyphal formation, with a low level of Ino80-Myc in the yeast state, which was significantly increased during hyphal initiation. The abundance of Ino80-Myc associated with HSG promoters peaked at 1.5 h and was maintained at a relatively high level during hyphal elongation (Figure 2a). Next, we evaluated the effects of Ino80 on the expression of HSGs during hyphal development. Compared with their expression in wild-type cells, the mRNA levels of *HWP1*, *ECE1*, and *ALS3* were dramatically reduced in the *ino80* strain during hyphal progression (Figure 2b). Consistent with the severe hyphal defective phenotype of the *ino80* mutant in YPD without serum, the association of Ino80 with *HWP1* promoter in YPD was weaker than that in YPD with serum. As expected, the *HWP1* expression level was also lower at 37°C without serum (Figure S2). As a control, we measured the transcription of *RAD18*, *RAD52*, and *PPH3*, which were involved in DNA-damage repair, during the hyphal program. The results showed that their expression was not affected by *INO80* deletion (Figure S3). To test whether Ino80 expression is regulated by yeast-hyphae morphological changes, we measured the mRNA and protein levels of Ino80 in the yeast and hyphae states. qRT-PCR results showed that the transcription levels of *INO80* were almost the same in the yeast and hyphal states (Figure 2c). Consistent with the qRT-PCR results, the Western blot results showed that the protein levels of Ino80 were comparable between the two states (Figure 2d). Collectively, we found that Ino80 was recruited to hypha-specific promoters and was involved in upregulating the expression of HSGs during the yeast-to-hyphae transition.

2.3 | Ino80 is required for eviction of H2A.Z from the hypha-specific promoters during hyphal development

Since *Ca*Ino80 has conserved structural features with *Sc*Ino80 and *Hs*Ino80 (Figure 1a), we speculated that *Ca*Ino80 contributed to hyphal formation by removing H2A.Z from the HSG promoters. To measure H2A.Z occupancy at HSG promoters, we performed ChIP-qPCR. H2A.Z was labeled with a FLAG tag at its C-terminus and expressed as driven by its own promoter. In contrast to the pattern of Ino80, H2A.Z quickly dissociated from these promoters during hyphal initiation and remained at a low level during hyphal development in wild-type cells (Figure 3a). However, dissociation of H2A.Z was not observed in the *ino80* deletion strain, as enrichment of H2A.Z at these promoters remained relatively constant across hyphal progression (Figure 3a). The dynamic association and dissociation of H2A.Z within these promoters were not attributable to a change in H2A.Z expression, since both the transcript and protein levels of *HTZ1*, which encodes H2A.Z in *ino80* cells, were similar to those in the wild type (Figure 3b,c). Interestingly, the expression levels of *HTZ1* were even higher in the hyphal state than in yeast cells (Figure 3b). As a control, the abundance of histone H3 associated with HSG promoters was not altered by the presence or absence of Ino80 (Figure 3d). Therefore, Ino80 mediated the removal of H2A.Z from hypha-specific promoters during hyphal development.

FIGURE 1 *Candida albicans* Ino80 is required for hyphal development. (a) Schematic comparison of *C. albicans* Ino80 (*Ca*Ino80), *Saccharomyces cerevisiae* Ino80 (*Sc*Ino80), and *Homo sapiens* INO80 (*Hs*INO80). (b) Cellular morphology of the wild type (WT, SN95), *htz1*, *swr1*, and *ino80* induced to form hyphae in the indicated liquid media conditions. (c) The percentage of hyphal cell and the length of hyphal cell after the wild type, *ino80*, *swr1*, and *htz1* inducing for 1 h and 3 h at 37°C, respectively. (d) Filamentous growth of the wild type and *ino80* mutant strain on Lee's and serum plates at 37°C. (e) Invasive growth of the wild type and *ino80* mutant strain on YPD plates. (f) The upper panel on the left side shows the truncated or mutated Ino80 variants and the lower panel shows the protein sequence alignment around the HSA domain of Ino80. (g) The Ino80 variants described in (f) were tested for complementing the hyphal defects of the *ino80* mutant strain. Scale bar, 20 μm.

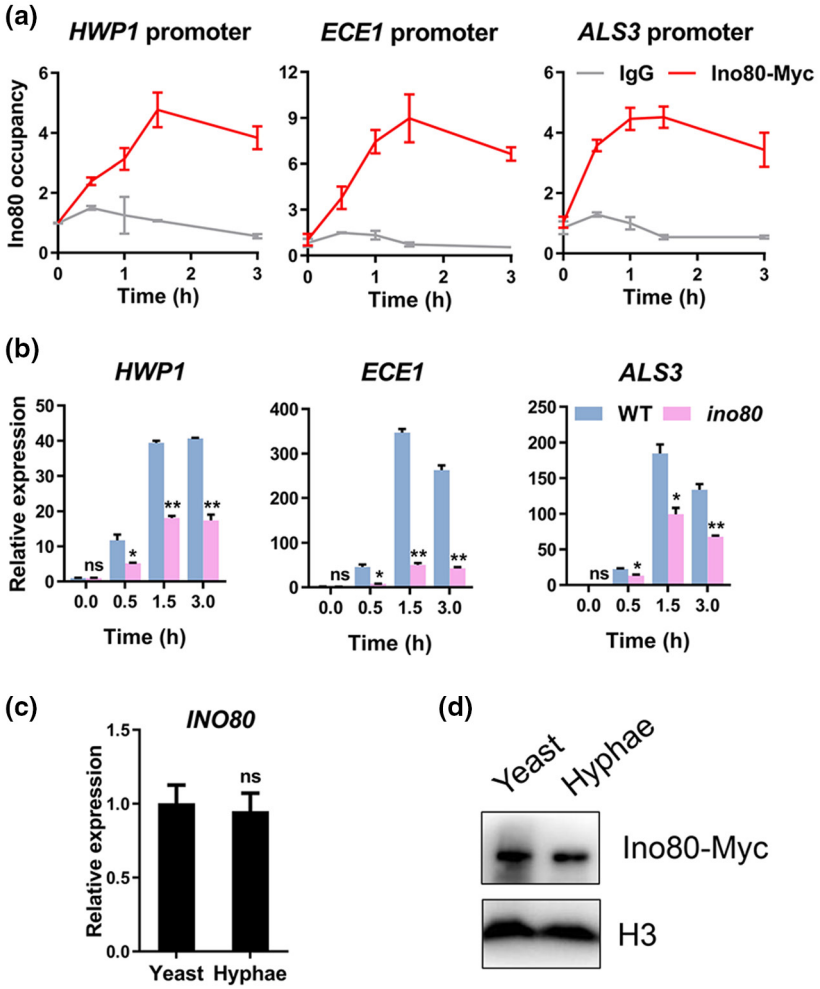

FIGURE 2 Ino80 is recruited to the promoters of HSGs and upregulates the expression of HSGs during hyphal development. (a) Dynamic occupancies of Myc-tagged Ino80 at promoters of *HWP1*, *ECE1*, and *ALS3* during hyphal development were analyzed by chromatin immunoprecipitation (ChIP) analysis. An overnight culture of cells containing Ino80-Myc were released into YPD with 10% serum, induced at 37°C, and harvested at indicated time. The samples were pulled down by anti-Myc antibodies and were amplified by quantitative PCR (qPCR) with primers targeting the promoters. Enrichment of Ino80-Myc was presented as a ratio of the target gene IP (bound/input). The signals obtained from IgG were used as control. The values from yeast cells of each strain were set to 1.00. (b) Transcription levels of *HWP1*, *ECE1*, and *ALS3* in wild-type and *ino80* mutant cells during hyphal induction. The cells were cultured in YPD with 10% serum at 37°C and collected at 0 h, 0.5 h, 1.5 h, and 3 h for quantitative reverse transcription PCR (qRT-PCR) analysis. The qRT-PCR values were normalized to *ACT1* values for each sample. (c) RT-qPCR comparison of *INO80* transcripts in wild-type yeast and hyphal cells. (d) Western-blot analysis of Ino80 protein levels in wild-type yeast and hyphal cells. The wild-type strain contains a copy of Ino80-Myc controlled by its own promoter. The Western blotting with anti-histone H3 antibody was used as loading control. The data show the average of three independent qPCR experiments (a, b, and c), with error bars representing the mean ± *SD*; $^{*}p < .05$, $^{**}p < .01$.

2.4 | Arp8 but not Arp5 is responsible for recruiting Ino80 to hypha-specific promoters and is required for hyphal development

All members of the INO80 family contain actin in combination with actin-related proteins (Arps) (Harata et al., 1999). Arp5 and Arp8, two unique components of the INO80 complex, interact with the ATPase and HAS domains of Ino80, respectively (Willhoft & Wigley, 2020; Yao et al., 2016), which are required for the recruitment of the INO80 complex to the DNA damage sites (Jonsson et al., 2004; Knoll et al., 2018). To determine whether Arp5 and Arp8 belong to the INO80 complex in *C. albicans*, we analyzed the interactions between Arp5 and Ino80 (Figure 4a) or Arp8 and Ino80 (Figure 4b) by reciprocal co-immunoprecipitation (Co-IP) experiments. Co-IP confirmed that both Arp5 and Arp8 were components of the INO80 complex. The roles of Arp5 and Arp8 in DNA double-strand break repair have been well-studied in mammalian and yeast cells (Kitayama et al., 2009; Shimada et al., 2008; van Attikum et al., 2004). Arp5 and Arp8 deletion mutants have a phenotype that mimics the Ino80 deletion mutant in DNA damage responses (Kashiwaba et al., 2010; Shimada et al., 2008). To investigate the functional roles of Arp5 and Arp8 in *C. albicans*, we compared the phenotypes of the three mutant cells in terms of hyphal formation (Figure 4c) and DNA damage responses (Figure 4d). Unexpectedly, Arp5 and Arp8 had distinct

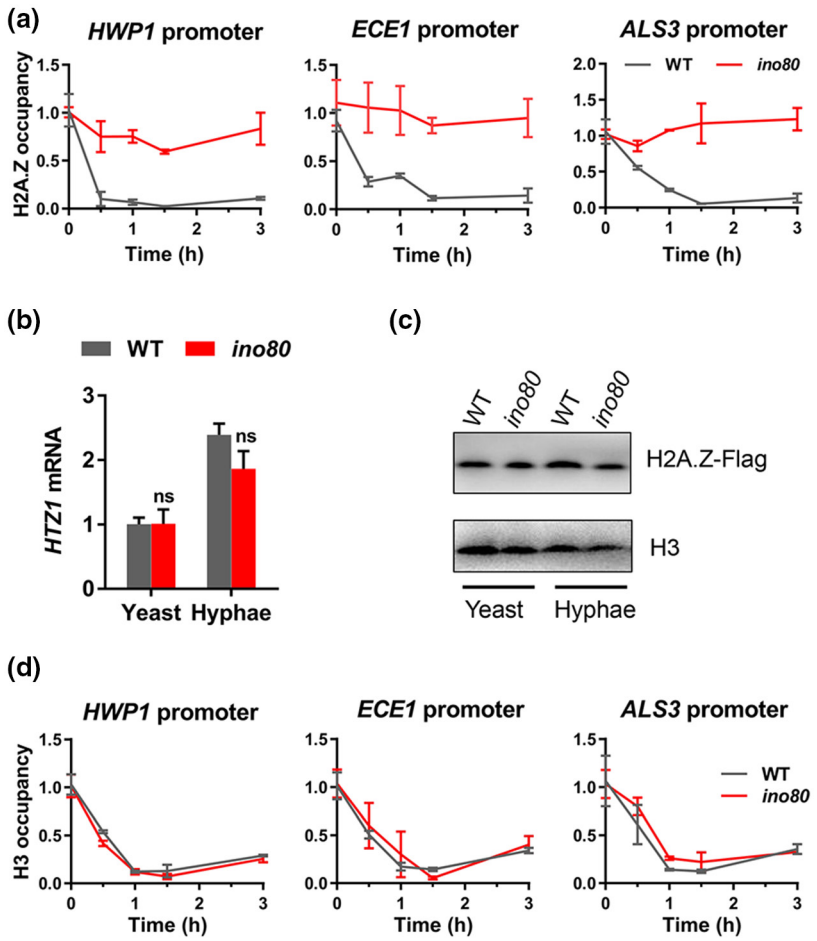

FIGURE 3 Ino80 is responsible for removing H2A.Z from HSG promoters during hyphal growth. (a) ChIP plus qPCR analysis of the FLAG-tagged H2A.Z in the wild type or *ino80* mutant cells at the promoters of hypha-specific genes *HWP1*, *ECE1*, and *ALS3* during hyphal induction. The qPCR values were presented as a ratio of the target gene IP (bound/input) and data from the overnight (0 h) samples were set to 1.0. (b) Comparison of *HTZ1* transcripts in wild-type and *ino80* mutant under yeast or hyphae growth conditions. Overnight cultures of the wild-type or *ino80* mutant cells were released into YPD for yeast growth (25°C, 3 h) or pre-warmed YPD plus 10% serum for hyphal induction (37°C, 3 h). The qRT-PCR values of *HTZ1* were normalized to the value of *ACT1* for each sample, and the value obtained from yeast samples was set to be 1.0. (c) Comparison of H2A.Z protein levels in wild-type and *ino80* mutant under yeast or hyphae growth conditions. H2A.Z-Flag controlled by its own promoter in wild-type and *ino80* mutant strains were analyzed by Western-blot with anti-Flag antibody. The anti-H3 antibody was used as loading control. (d) The occupancies of H3 at promoters of *HWP1*, *ECE1*, and *ALS3* during hyphal induction were measured by ChIP-qPCR. Mean ± *SD* values from two independent experiments are shown; $^{*}p < .05$.

effects on hyphal formation in *C. albicans*. Deletion of *ARP8* impaired the hyphal program of *C. albicans* and resulted in a phenotype similar to that of the *ino80* mutant strain. Both *arp8* and *ino80* mutant cells showed defective filament formation. However, the deletion of *ARP5* had subtle effects on hyphal development and resulted in a phenotype similar to that of the wild-type strain (Figure 4c). During DNA damage response, Arp5 and Arp8 share the same function as Ino80. Wild-type, *ino80*, *arp5*, and *arp8* cells were serially diluted and spotted onto YPD plates containing 40 mM hydroxyurea (HU) or 0.03% methyl methanesulfonate (MMS). All three mutants (*ino80*, *arp5*, and *arp8*) were hypersensitive to DNA-damaging agents (Figure 4d). Reintroduction of ectopically expressed *INO80*, *ARP5*, or *ARP8* into *ino80*, *arp5*, or *arp8* mutant cells, respectively, rescued their growth defects in response to DNA damage treatment (Figure 4d). We further examined the expression levels of the DNA damage-specific gene *RAD18* during DNA damage treatment (Feng et al., 2020) and the hypha-specific gene *HWP1* during hyphal development in wild-type, *ino80*, *arp5*, and *arp8* mutant cells. After treatment with the DNA damage agents, *RAD18* expression levels were lower in all three mutant cells than in wild-type cells (Figure 4e). During hyphal development, the induction of *HWP1* expression was inhibited in *ino80* and *arp8* mutant cells, but not in *arp5* mutant cells (Figure 4f). Expression patterns correlated with the phenotypes of the three mutants. To clarify the discrepancy between Arp5 and Arp8 during hyphal formation and DNA damage response, we evaluated the contribution of Arp5 and Arp8 to Ino80 recruitment using ChIP-qPCR. Deleting either *ARP5* or *ARP8* prevented Ino80 from binding to the *RAD18* promoter during DNA damage stimulation (Figure 4e). However, deletion of *ARP8*, but not *ARP5*, blocked the Ino80 binding to the *HWP1* promoter during hyphal induction (Figure 4f).

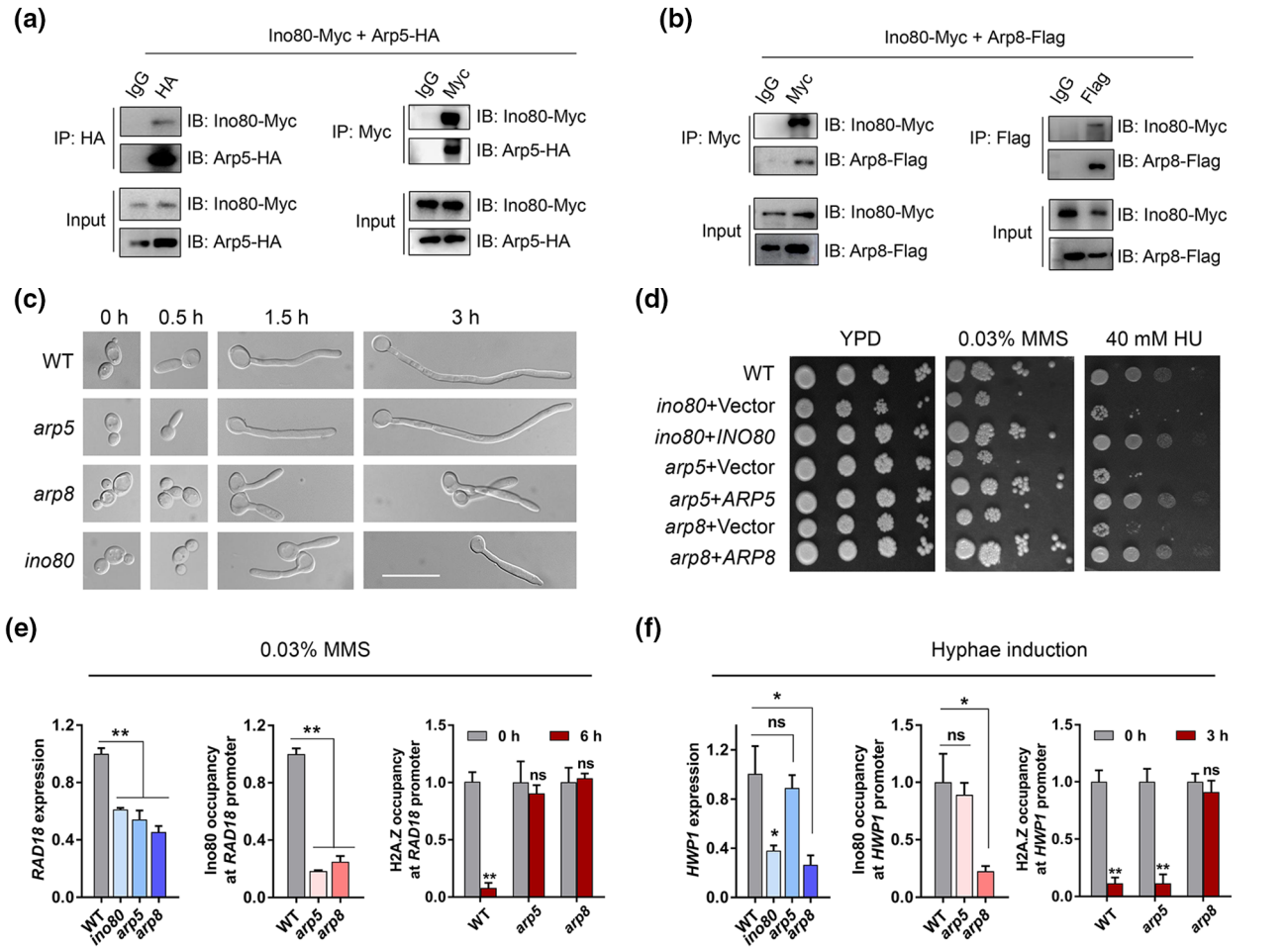

FIGURE 4 Distinct roles of Arp5 and Arp8 in regulating DNA damage response and hyphal development of *Candida albicans*. (a) Interaction between the Ino80 and Arp5. Cell lysates from the cells expressing both Ino80-Myc and Arp5-HA were pulled down with the polyclonal anti-HA or anti-Myc antibody and then probed with monoclonal antibodies against Myc or HA. Immunoprecipitating with IgG was used as a negative control. (b) Interaction between the Ino80 and Arp8. Cell lysates from cells expressing both Ino80-Myc and Arp8-Flag were pulled down with the polyclonal anti-Myc or anti-Flag antibody. Ino80-Myc and Arp8-Flag were detected by Western blot by using monoclonal antibodies against Myc and Flag. (c) Cell morphology of the wild-type, *ino80*, *arp5*, and *arp8* strains. The overnight culture of these strains was induced in YPD + 10% serum media at 37°C to form hypha. Scale bar represents 20 μm. (d) Dot assays of the *ino80*, *arp5*, and *arp8* mutant strains after MMS and HU treatment. Cells of wild-type, *ino80*, *arp5*, *arp8*, and the revertant strains were serially diluted (10-fold) and spotted onto YPD plates containing 0.03% MMS or 40 mM of HU. The plates were incubated at 25°C for 3 days. (e) DNA damage response assays. The expression levels of *RAD18* were analyzed by qRT-PCR. Log-phase cells of the wild-type, *ino80*, *arp5*, and *arp8* mutant strains were stimulated by 0.03% MMS and harvested after 6 h at 25°C. The signal obtained from *ACT1* was used for normalization and the expression values in the wild type were set to 1.0. The Ino80 abundance on the *RAD18* promoter was analyzed by ChIP-qPCR. The wild-type, *arp5*, and *arp8* cells carrying Ino80-Myc were cultured in YPD containing 0.03% MMS. The values were presented as a ratio of the target gene IP (bound/input). The signals obtained from the wild type were normalized to be 1.0. H2A.Z occupancy at the *RAD18* promoters of wild-type, *arp5*, and *arp8* mutants was quantified by ChIP-qPCR after treatment with 0.03% MMS. (f) Hyphal development analysis. The expression levels of *HPW1* in the wild-type, *ino80*, *arp5*, and *arp8* mutant cells induced in YPD + 10% serum were analyzed by using qRT-PCR. The Ino80 abundance on the *HWP1* promoter was determined by ChIP-qPCR. The wild-type, *arp5*, and *arp8* cells carrying Ino80-Myc were induced for hyphal growth. H2A.Z occupancy at the *HWP1* promoters of wild-type, *arp5*, and *arp8* mutant cells was quantified by ChIP-qPCR after inducing hyphal growth conditions. The data show the average of three independent experiments (e and f), with error bars representing the mean ± *SD*; $^{*}p < .05$, $^{**}p < .01$.

Therefore, Arp5 and Arp8 were both required for the recruitment of Ino80 to DNA damage-specific promoters, whereas only Arp8 was required for the recruitment of Ino80 to hypha-specific promoters. In line with the Ino80 occupancy at the *RAD18* promoter, H2A.Z was efficiently removed from the *RAD18* promoter in the wild-type cells, but not in the *arp5* or *arp8* mutant cells after treatment with the DNA damage agents (Figure 4e). Consistently, H2A.Z was removed from the *HWP1* promoters in the wild-type and *arp5* mutant cells, but not in the *arp8* mutant cells during hyphal induction (Figure 4f). These results indicated that Arp5 and Arp8 were two subunits of the INO80 complex in *C. albicans* and played distinct roles in different cellular processes. The two subunits were all involved in DNA

damage responses, whereas only Arp8, but not Arp5, was required for hyphal development in *C. albicans*.

Brg1 is a key transcription factor required for hyphal elongation in *C. albicans* (Cleary et al., 2012; Lu et al., 2012). Deletion of Brg1 resulted in a phenotype similar to that of the *ino80* mutant during hyphal elongation; thus, we examined the role of Brg1 in the recruitment of Ino80 to hypha-specific promoters. As expected, loss of Brg1 completely abolished Ino80 occupancy in the *HWP1* promoter (Figure S4a). These showed that the binding of Ino80 with hypha-specific promoters not only relied on the INO80 complex-specific subunit Arp8 but also required the existence of the transcription factor Brg1. Considering the opposing roles of Ino80 and Swr1 in hyphal formation of *C. albicans*, we analyzed the dynamic occupancy of Ino80 and Swr1 on the *HWP1* promoter in wild-type cells by ChIP-qPCR (Figure S4b). The promoter-associated Ino80-Myc maintained at a low level in the yeast state significantly increased during hyphal initiation and remained associated during hyphal elongation, which is in line with the Brg1 recruiting dynamics in previous studies (Lu et al., 2012). In contrast to Ino80, Swr1-Myc was strongly associated with the *HWP1* promoter in yeast cells, dissociated quickly from the promoter during hyphal initiation, and remained unbound during hyphal development. Recruitment of Ino80 and departure of Swr1 were dynamically coordinated during hyphal induction in *C. albicans*.

2.5 | Ino80 contributes to the pathogenicity of *C. albicans* during systemic infection

As a commensal fungus in the human microbiota, *C. albicans* infection can cause severe problems in immunodeficient and compromised individuals (Whiteway & Bachewich, 2007). It is widely accepted that the morphological transition from yeast to hyphae is a major contributor to *C. albicans* virulence (Lo et al., 1997). In view of the above observations, the *ino80* null mutant strain has a deficiency in the yeast-to-hyphae transition. We next examined the virulence of the *ino80* mutant cells using a mouse model of systemic infection. Mice inoculated with 5×10^6 wild-type cells died within 7 days, and a lower inoculum of 5×10^5 cells led to the death of all mice within 15 days (Figure 5a). However, in the group of mice infected with *ino80* mutant cells, all mice survived for more than 20 days in both inoculum sizes (Figure 5a). Thus, the *ino80* mutant was found to be avirulent in mice.

To analyze the impact of growth defects on the virulence of the *ino80* mutant strain, we compared the growth rates of wild-type and *ino80* mutant cells. The deletion of *INO80* slightly reduced the cell growth rate in solid or liquid YPD media (Figure S5). Therefore, the avirulent phenotype of the *ino80* mutant in systemic infection of mice might be a combination of morphological and growth defects. The kidney is a major target organ of invasive candidiasis (Parker et al., 1976), where hyphae formation can cause severe tissue damage, resulting in host death; therefore, observation of early morphogenesis and clearance of *C. albicans* would be a direct way to measure virulence (Zhu et al., 2021). To determine whether the attenuated virulence of the *ino80* strain was due to its morphological defect, we carried out periodic acid–Schiff (PAS) staining of the kidney sections from the *C. albicans-infected* mice, which came from mice infected with 1×10^6 cells of the wild-type or *ino80* strain on days 1, 2, and 7. Wild-type cells formed hyphae in the kidney 1 day after inoculation, followed by the development of massive, long filaments over time (Figure 5b). The *ino80* cells remained in yeast form after 1 day of infection and only formed short filaments after 2 days of infection. The *ino80* cells were almost cleared and were hardly observed 7 days post-infection (Figure 5b). To assess the survival ability of the *ino80* deletion cells in the host, we evaluated the fungal burden in the mouse kidney and liver after 2 days of infection with 1×10^6 cells. Kidneys from mice infected with the wild-type strain contained more *C. albicans* cells than those infected with the *ino80* strain (Figure 5c). The fungal load of wild-type cells was also significantly higher than that of *ino80* cells in the liver (Figure 5c). The host immune system is the major defense against *C. albicans* infection (Cheng et al., 2012); therefore, we checked the survival ability of *ino80* cells in immune cells by co-incubating wild-type and *ino80* cells with the murine macrophage cell line RAW264.7. The supernatants of the co-cultures were diluted and spread on YPD plates to observe the survival of *C. albicans* cells. After 6 h of co-incubation, the *ino80* mutant cells were almost completely cleared by macrophages, whereas 20% of the wild-type cells were still alive (Figure 5d). We also measured the release of lactate dehydrogenase (LDH) in the supernatant to represent damage to immune cells after infection with *C. albicans*. LDH release was significantly lower in the supernatant incubated with *ino80* cells than in the supernatant incubated with wild-type cells (Figure 5e), suggesting that the *ino80* mutant strain causes less damage to immune cells. Altogether, we concluded that Ino80 contributed to the pathogenicity of *C. albicans* during systemic infection and might be a candidate target for antifungal therapy.

3 | DISCUSSION

ATP-dependent chromatin remodelers regulate various biological functions, such as the DNA damage response, telomere integrity, and gene expression (Smith & Peterson, 2005). In this study, we demonstrated that Ino80, the core enzyme of the INO80 complex, was recruited to the promoters of HSGs and regulated the expression of HSGs by removing H2A.Z from the nucleosome, which facilitated hyphal development in *C. albicans*. Furthermore, the unique subunit of the INO80 complex, Arp8, was responsible for recruiting Ino80 to the promoters of HSGs. Deleting Arp8 results in Ino80 being unable to bind the promoter regions of HSGs and attenuate the expression of HSGs (Figure 6). In addition, we also demonstrated that Arp5, another unique subunit of the INO80 complex, did not contribute to hyphal formation but was required for DNA damage responses. Therefore, the diverse roles of the INO80 complex in different biological processes are mediated by its different components in response to distinct stimuli.

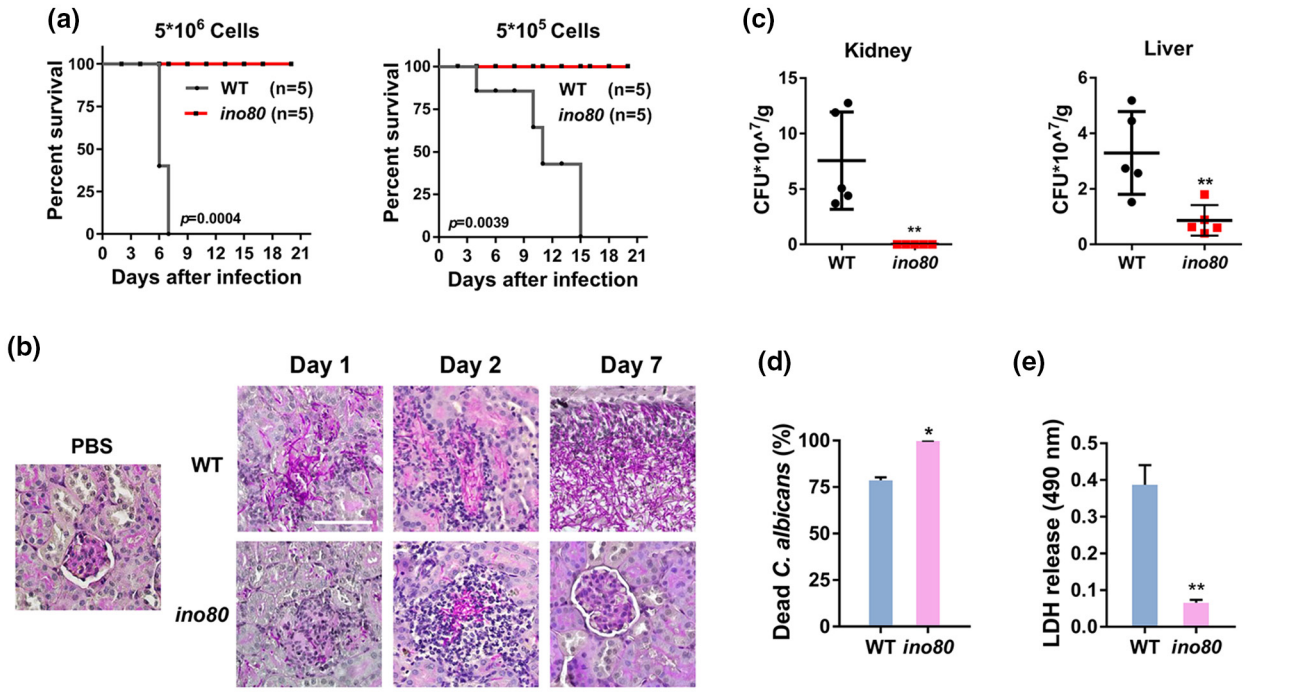

FIGURE 5 Ino80 contributes to the virulence of *Candida albicans*. (a) Survival kinetics of mice intravenously injected with 5×10^6 (high dose) or 5×10^5 (low dose) of the wild-type or *ino80* mutant cells. The survival of the mice was monitored daily, and the log-rank test was used to analyze the statistical significance of the survival correlations between groups. (b) Kidneys from the mice infected by 1×10^5 of the wild-type, *ino80* mutant cells, or PBS were collected 1 day, 2 days, or 7 days post-infection. Then, the tissues were fixed, sectioned, and stained with periodic acid–Schiff (PAS) reagent to visualize fungal cells. Scale bar represents 20 μm. (c) Recoverable fungal colony-forming units (CFUs) in infected mouse kidney and liver were determined after 2 days of inoculation with the indicated *C. albicans* strains (5 mice each strain). Each data point represents the CFU/g of kidney or liver from individual mice of each category. An unpaired, two-tailed Student's *t*-test was used for two-group comparisons, $^{**}p<.01$. (d and e) Primary murine-macrophage RAW264.7 cells were co-cultured with the wild-type or *ino80* strain at a multiplicity of infection (Ghazwani et al., 2021) of 1 for 6 h. Fungal survival was calculated according to the number of colonies after spreading the diluted supernatant culture medium to YPD plates without lysate the macrophage. Macrophage death was assessed based upon lactate dehydrogenase (LDH) release. Results are reported as mean ± *SD* from triplicate experiments and an unpaired, two-tailed Student's *t*-test was used for two-group comparisons (c); $^{*}p<.05$, $^{**}p<.01$, $^{***}p<.001$.

As specific components of the INO80 complex, both Arp5 and Arp8 are required for INO80 ATPase activity, since losing either Arp5 or Arp8 compromises the ATPase activity of INO80 and displays an INO80 deletion morphology (Shen et al., 2003). Structural analysis proved that lack of Arp5 or Arp8 does not affect the integrity of the entire INO80 complex, indicating that both proteins have less impact on structural integrity than on the process of chromatin remodeling (Knoll et al., 2018). In this study, we found that Ino80 recruitment at the HSG promoter relied on Arp8 but not on Arp5. However, similar to the function of Ino80, both Arp5 and Arp8 are essential for *C. albicans* growth after stimulation with DNA-damaging agents. The reason for this discrepancy may be that Arp5 is indispensable for Ino80 recruitment during DNA-damage repair but not during hyphal formation. Recent studies in *Arabidopsis* have also demonstrated that ARP5 functions together with INO80 to cope with replication stress and to mediate plant cellular proliferation (Jha & Dutta, 2009). ARP5 is not required for INO80-mediated flowering time control and related gene transcription (Kang et al., 2019). These observations suggest that although Arp5 is essential for the activity of the INO80 complex in DNA-damage repair, it may function less in some specific growth processes. In addition, besides being a component of the INO80 complex, a high quantity of Arp5 was also found in another separate subcomplex from sucrose gradient separation in yeast, which indicated that Arp5 might play multi roles in vivo (Yao et al., 2016). The transcription factor Brg1 is recruited to the promoter regions of HSGs and regulates hyphal development (Lu et al., 2012). We demonstrated that Brg1 was required for recruiting Ino80 to promoters of HSGs during yeast to hyphae transition, implying the contribution of other factors as a "recruiter" for the recruitment of the INO80 complex to some sequence-specific regions.

As an opportunistic fungal pathogen in humans, *C. albicans* can cause serious infections in immunocompromised individuals (Brown et al., 2012). Our results highlight the crucial role of Ino80 in the pathogenesis of *C. albicans* during systemic infections. *C. albicans* without Ino80 is avirulent in mice and causes less immune cell damage. In line with this, in our study, *ino80* mutant cells were more effectively cleared by host immune cells compared to wild-type cells. We propose that Ino80 is a potential target for antifungal treatment. To our knowledge, this is the first study to elucidate the function of Ino80 in *C. albicans*.

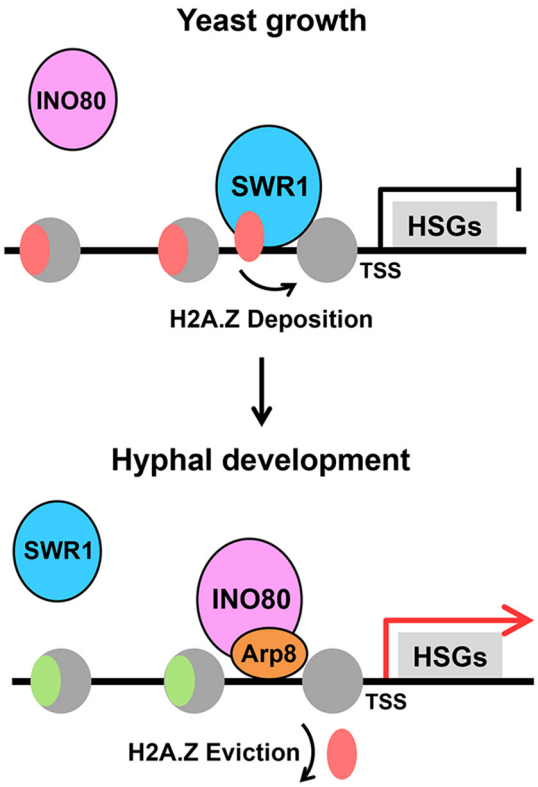

FIGURE 6 Model of INO80 and SWR1 complexes regulated exchange of H2A.Z during hyphal development of *Candida albicans*. The exchange of histone variants is known to regulate the morphological transitions in *C. albicans*. In yeast state, the SWR1 complex mediates H2A.Z deposition in the nucleosomes of hypha-specific promoters to prevent nucleosome removal, which in turn inhibits the expression of hypha-specific genes. During hyphal induction, the SWR1 complex is departure from the promoters and the INO80 complex is recruited to these regions via Arp8 subunit. Then, Ino80 plays a vital role in removing H2A.Z from these promoters, thereby activating the transcription of hypha-specific genes and facilitating yeast to hyphae transition.

4 | EXPERIMENTAL PROCEDURES

4.1 | Strains and growth conditions

All strains used in this study are listed in Table S1. Plasmid constructs used in this study are listed in Table S2. *Candida* strains were routinely maintained in yeast extract-peptone-dextrose (YPD, 2% BD Difco peptone, 2% dextrose, 1% yeast extract) agar, and were routinely grown on liquid YPD overnight prior to each experiment or on synthetic complete medium SCD (0.17% Difco yeast nitrogen base w/o ammonium sulfate, 0.5% [37 mM] ammonium sulfate, auxotrophic supplements, and 2% dextrose) for selection of prototrophic strains. *C. albicans* SN95 was used as wild type, and the deletion strains relating to *INO80* were derived from SN148, *HTZ1*, and *ARP5*-associated strains were derived from SN152. The construction of these strains was using PCR-based homolog recombination (Noble & Johnson, 2005). To rescue the phenotype of the *INO80* deletion strain, DNA fragments containing the full-length wild-type, *INO80*, *INO80* ΔN, *INO80* ΔC, and *INO80*-K704R were cloned into the plasmid of pCPC20 (Chang et al., 2015). Then, these plasmids were linearized using primers of Cap22 and Cap23 by PCR amplification and integrated at the *ADE2* locus of the genome. The right integration was confirmed by PCR. All primer sequences used for strains and plasmids construction are listed in Table S3. Hyphal inductions were performed as follows. Strains were grown overnight in liquid YPD at 25°C, pelleted, washed with PBS twice, resuspended in an equal volume of PBS, and diluted in preheated (37°C) YPD medium with or without 10% serum in a ratio of 1:200.

4.2 | Spot assays

Cells were grown in liquid YPD culture to log phase, and cell density was measured using a hemocytometer and adjusted to 1×10^7 cells per milliliter. Five-fold serial dilutions were prepared. Diluted cells were stamped onto freshly prepared YPD agar plates with or without 0.03% methyl methane sulphonate (MMS) or 40 mM hydroxyurea (HU). MMS or HU sensitivity was determined after incubation at 30°C for 2 days.

4.3 | Western blot

C. albicans was pelleted and washed in sterile water once. Then, adding quantified RIPA lysis buffer (50 mM Tris–HCl [pH 7.4], 150 mM NaCl, 1 mM EDTA, 1% Triton X-100, 1% sodium deoxycholate, 0.1% SDS) containing PMSF (Sigma-Aldrich) and Cocktail (Perbio Science) with 5 × loading buffer (300 mM Tris–HCl [pH 6.8], 10% SDS, 0.05% bromophenol blue, 2 mM EDTA) to resuspended the pellets. Boiling at 95°C for 10 min to lysate cells before loading to the gel.

4.4 | Quantitative reverse transcription PCR (qRT-PCR)

Extracting the RNA of *C. albicans* cells was performed as before (Collart & Oliviero, 1993). 1 mg of RNA was reverse-transcribed to 200 μl cDNA following the instruction (FastKing RT Kit with gDNase, KR116-02, Tiangen). 2.5 μl of cDNA was used per 10 μl qRT-PCR reaction with either primers of *HWP1* or other target genes described in Table S3. Samples were prepared according to the manufacturer's recommendations (qPCR SyGreen 2-Step Detect Lo-ROX; FP205-02, Tiangen) and real-time quantitative PCR was conducted on a Roche Light cycler 96 real-time PCR detection system with the following program: initial melting occurred at 94°C for 300 s, followed by 40 cycles of melting at 95°C for10s followed by annealing at 58°C for 10 s then extension at 72°C for 25 s with fluorescent measurements taken at the end of each extension. Melt curves (60°C–94°C) with continuous acquisition were generated to verify single product.

4.5 | Chromatin immunoprecipitation (ChIP)

ChIP assays were performed as previously described (Kim & Lee, 2020) with some modifications. Briefly, *C. albicans* cells were crosslinked with 1% formaldehyde and suspended in 1 ml Spheroplasting buffer (1 M sorbitol, 50 mM Tris–Cl [pH 7.4]) with 10 μl β-mercaptoethanol (final 5 mM) and 5 μl zymolyase (final 500 mg, 10 units) and mixed by vortex. Incubating cells at 30°C for 30 min. Wash with 500 μl Lysis buffer (50 mM HEPES [pH 7.5], 150 mM NaCl, 1 mM EDTA, 1% Triton X-100, 0.1% Na-Deoxycholate, 1 mM PMSF, protease inhibitors cocktail) twice and the pellet cells were resuspended in 500 μl Lysis buffer. Sonicate the spheroplasts using a microtip probe in a sonicator ten times for 30 s on/30 s off. Cross-linked chromatin fragments were immunoprecipitated with antibodies that specifically recognized anti-MYC (sc-40, Santa Cruz Biotechnology), anti-FLAG M2 (F1804, Sigma), or HA-probe (F-7) (sc-7392, Santa Cruz Biotechnology). 10 μl protein A/G PLUS-Agarose beads (sc-2003, Santa Cruz Biotechnology) were added into each sample and the immunoprecipitated complexes were washed gradually with sequentially: once in Lysis buffer, twice in W2 buffer (50 mM HEPES (pH 8.0), 1 M NaCl, 1 mM EDTA (pH 0.8), 1% Triton X-100, 0.1% Sodium deoxycholate), once in W3 buffer (10 mM Tris–HCl (pH 8.0), 125 mM LiCl, 0.5% NP-40, 0.5% Sodium deoxycholate, 1 mM EDTA (pH 8.0) PK buffer: 100 mM Tris–HCl (pH 7.5), 12.5 mM EDTA, 150 mM NaCl, 1% SDS), and once in TE buffer (10 mM Tris–HCl (pH 8.0), 1 mM EDTA). Next, the immunoprecipitated complexes were eluted from beads with elution buffer (10 mM Tris–HCl pH 8.0, 1 mM EDTA, 1% SDS). Formaldehyde cross-linking was reversed by incubating the eluates at 65°C, 10 h. Eluted DNA was treated with 100 μg/ml proteinase K (Invitrogen) and purified with QIAquick PCR purification Kit (Qiagen). Immunoprecipitated fractions and WCEs containing DNA were analyzed by qPCR.

4.6 | Mouse infection models

For analysis of the virulence of the *INO80* deletion cells in vivo, the wild-type (SN95), and *ino80* strains were inoculated from overnight cultures 1:50 into fresh YPD medium and grew for 6 h at 30°C. Logarithmically growing cells were pelleted, washed twice with PBS, and counted with a hemocytometer. For the disseminated candidiasis model, male ICR mice, housed under specific pathogen-free conditions, were systemically infected by intravenous injection with 5×10^5 or 5×10^6 of the wild-type or *ino80* cells (in 0.1 ml PBS), respectively, each group containing 5 mice. The survival of mice was monitored daily. To access the fungal burden in organs, the mice with weight ranging from 18 to 20 g were euthanized 2 days after infection. Kidneys and livers were isolated and weighed. Then, these organs were homogenized in PBS and serially diluted before plated onto YPD agar plate. Fungal colony-forming units were counted after incubation at 30°C for 48 h. All animal experiments were approved by the Institutional Animal Care and Use Committee (IACUC) of Shanghai Institute of Biochemistry and Cell Biology, Chinese Academy of Sciences, and complied with all relevant ethical regulations.

4.7 | Periodic acid–Schiff (PAS) staining

Male ICR mice were infected with 1×10^6 of the wild-type (SN95, $n = 5$) or *ino80* ($n = 5$) cells as described above. Following 7 days, animals were euthanized on days 1, 2, and 7. Then, the kidneys were isolated and fixed in 4% paraformaldehyde (PFA) at room temperature for 12 h. Fixed tissues were processed in serials of ethanol to dehydration and xylenes (histological grade; twice for 40 min each), followed by transfer to melted paraffin wax (Sigma) for 2 h at 65°C. Paraffin blocks were prepared and 4 μm sections were made. Periodic acid–Schiff (PAS) staining was performed as previously described (Baum, 2008).

4.8 | Survival ability assay of *C. albicans* cells in macrophages and their ability to damage macrophages

RAW264.7 mouse macrophages (1.5×10^4) were inoculated into 96-well plates and challenged with *C. albicans* at a multiplicity of infection (Ghazwani et al., 2021) of 1. After 6 h of coincubation at 37°C with 5% CO_2, the engulfment by macrophages was checked by spreading the culture medium on YPD plates with 100-fold dilutions. The CFUs were counted, and survival was normalized to *C. albicans* controls incubated in the absence of immune cells. To investigate the damage potent of different *C. albicans* strains, the lactate dehydrogenase (LDH) in the surrounding co-culture medium were measured according to the instruction of the LDH cytotoxicity assay kit (C0016, Beyotime Biotechnology). Briefly, RAW264.7 cells were cultured to 95% confluence in the 96-well culture plate. The cells were challenged with PBS or the wild-type (SN95), *ino80* strain (MOI 1), and incubated in the humidified 37°C incubator containing 5% CO_2 for 6 h. Afterward, the culture supernatant was collected for the LDH assay. LDH transfers NAD to NADH, which could be detected by colorimetric (490 nm) assay specifically. Based on the manufacturer's instructions, a standard curve was generated and the sample values were estimated from the curve. The experiment was performed in triplicate.

4.9 | Statistical analysis

The data were presented as mean ± *SD*. A two-tailed unpaired Student's *t*-test was performed to compare the differences between treated groups relative to their paired controls. A log-rank test was used to analyze the statistical significance of survival correlations between groups (*$p < .05$, **$p < .01$, ***$p < .001$). Statistical analyses were performed using GraphPad Prism 7.04 (GraphPad Software, Inc.).

AUTHOR CONTRIBUTIONS

JC and WZ supervised the study. QZ, WZ, and JC designed the experiments. QZ performed the experiments. QZ, WZ, and JC analyzed the data. BD and HW provided technical support. QZ, WZ, and JC wrote the manuscript.

ACKNOWLEDGMENT

This work was financially supported by grants from the National Natural Science Foundation of China (Nos. 31970144 and 32170196).

CONFLICT OF INTEREST

The authors have declared that no competing interests exist.

ETHICS STATEMENT

All animal experiments were approved by the Institutional Animal Care and Use Committee (IACUC) of Shanghai Institute of Biochemistry and Cell Biology, Chinese Academy of Sciences and complied with all relevant ethical regulations.

DATA AVAILABILITY STATEMENT

The data supporting the findings of this study are available from the corresponding author upon reasonable request.

ORCID

Wencheng Zhu https://orcid.org/0000-0001-8123-9504
Jiangye Chen https://orcid.org/0000-0002-8564-6438

REFERENCES

Alatwi, H.E. & Downs, J.A. (2015) Removal of H2A.Z by INO80 promotes homologous recombination. *EMBO Reports*, *16*, 986–994.

van Attikum, H., Fritsch, O., Hohn, B. & Gasser, S.M. (2004) Recruitment of the INO80 complex by H2A phosphorylation links ATP-dependent chromatin remodeling with DNA double-strand break repair. *Cell*, *119*, 777–788.

Bailey, M.R., Ansoborlo, E., Chazel, V., Fritsch, P., Hodgson, A., Kreyling, W.G. et al. (2004) Radionuclide biokinetics database (RBDATA-EULEP): an update. *Radiation Protection Dosimetry*, *112*, 535–536.

Baum, S. (2008) The PAS reaction for staining cell walls. *CSH Protocols*, *2008*, pdb prot4956.

Becker, P.B. & Horz, W. (2002) ATP-dependent nucleosome remodeling. *Annual Review of Biochemistry*, *71*, 247–273.

Brown, G.D., Denning, D.W., Gow, N.A.R., Levitz, S.M., Netea, M.G. & White, T.C. (2012) Hidden killers: human fungal infections. *Science Translational Medicine*, *4*. https://doi.org/10.1126/scitranslmed.3004404

Cao, L.L., Ding, J., Dong, L.G., Zhao, J.Y., Su, J.M., Wang, L.Y. et al. (2015) Negative regulation of p21(Waf1/Cip1) by human INO80 chromatin remodeling complex is implicated in cell cycle phase G2/M arrest and abnormal chromosome stability. *PLoS One*, *10*. https://doi.org/10.1371/journal.pone.0137411

Chakraborty, P. & Magnuson, T. (2022) INO80 requires a polycomb subunit to regulate the establishment of poised chromatin in murine spermatocytes. *Development*, *149*. https://doi.org/10.1242/dev.200089

Chang, P., Fan, X.Y. & Chen, J.Y. (2015) Function and subcellular localization of Gcn5, a histone acetyltransferase in *Candida albicans*. *Fungal Genetics and Biology*, *81*, 132–141.

Cheng, S.C., Joosten, L.A.B., Kullberg, B.J. & Netea, M.G. (2012) Interplay between *Candida albicans* and the mammalian innate host defense. *Infection and Immunity*, *80*, 1304–1313.

Clapier, C.R., Iwasa, J., Cairns, B.R. & Peterson, C.L. (2017) Mechanisms of action and regulation of ATP-dependent chromatin-remodelling complexes. *Nature Reviews Molecular Cell Biology*, *18*, 407–422.

Cleary, I.A., Lazzell, A.L., Monteagudo, C., Thomas, D.P. & Saville, S.P. (2012) BRG1 and NRG1 form a novel feedback circuit regulating *Candida albicans* hypha formation and virulence. *Molecular Microbiology*, *85*, 557–573.

Collart, M.A. & Oliviero, S. (1993) Preparation of yeast RNA. *Current Protocols in Molecular Biology*, *23*, 13.12.11–13.12.15.

Dalle, F., Wachtler, B., L'Ollivier, C., Holland, G., Bannert, N., Wilson, D. et al. (2010) Cellular interactions of *Candida albicans* with human oral epithelial cells and enterocytes. *Cellular Microbiology*, *12*, 248–271.

Drengk, A., Fritsch, J., Schmauch, C., Ruhling, H. & Maniak, M. (2004) Site directed disassembly of filamentous actin reveals a specific function for the endosomal actin coat in amoebae. *European Journal of Cell Biology*, *83*, 43.

Ebbert, R., Birkmann, A. & Schuller, H.J. (1999) The product of the SNF2/SWI2 paralogue INO80 of *Saccharomyces cerevisiae* required for efficient expression of various yeast structural genes is part of a high-molecular-weight protein complex. *Molecular Microbiology*, *32*, 741–751.

Eustermann, S., Schall, K., Kostrewa, D., Lakomek, K., Strauss, M., Moldt, M. et al. (2018) Structural basis for ATP-dependent chromatin remodelling by the INO80 complex. *Nature*, *556*, 386–390.

Feng, J.R., Islam, A., Bean, B., Feng, J., Sparapani, S., Shrivastava, M. et al. (2020) Hof1 plays a checkpoint-related role in MMS-induced DNA damage response in *Candida albicans*. *Molecular Biology of the Cell*, *31*, 348–359.

Ghazwani, M., Hani, U., Osmani, R.A.M., Rahamathulla, M., Begum, M.Y., Wahab, S. et al. (2021) An efficient herbal approach for treating fungal infection in cervical cancer patients by developing and optimizing a vaginal suppository. *International Journal of Polymer Science*, *2021*, 1–11.

Gow, N.A.R., van de Veerdonk, F.L., Brown, A.J.P. & Netea, M.G. (2012) *Candida albicans* morphogenesis and host defence: discriminating invasion from colonization. *Nature Reviews. Microbiology*, *10*, 112–122.

Guan, Z.Y. & Liu, H.P. (2015) Overlapping functions between SWR1 deletion and H3K56 acetylation in *Candida albicans*. *Eukaryotic Cell*, *14*, 578–587.

Harata, M., Oma, Y., Mizuno, S., Jiang, Y.W., Stillman, D.J. & Wintersberger, U. (1999) The nuclear Actin-related protein of *Saccharomyces cerevisiae*, Act3p/Arp4, interacts with core histones. *Molecular Biology of the Cell*, *10*, 2595–2605.

Jha, S. & Dutta, A. (2009) RVB1/RVB2: running rings around molecular biology. *Molecular Cell*, *34*, 521–533.

Jonsson, Z.O., Jha, S., Wohlschlegel, J.A. & Dutta, A. (2004) Rvb1p/Rvb2p recruit Arp5p and assemble a functional Ino80 chromatin remodeling complex. *Molecular Cell*, *16*, 465–477.

Kang, H.J., Zhang, C., An, Z.X., Shen, W.H. & Zhu, Y. (2019) AtINO80 and AtARP5 physically interact and play common as well as distinct roles in regulating plant growth and development. *The New Phytologist*, *223*, 336–353.

Kashiwaba, S., Kitahashi, K., Watanabe, T., Onoda, F., Ohtsu, M. & Murakami, Y. (2010) The mammalian INO80 complex is recruited to DNA damage sites in an ARP8 dependent manner. *Biochemical and Biophysical Research Communications*, *402*, 619–625.

Kim, J. & Lee, J.S. (2020) Rapid method for chromatin immunoprecipitation (ChIP) assay in a dimorphic fungus, *Candida albicans*. *Journal of Microbiology*, *58*, 11–16.

Kitayama, K., Kamo, M., Oma, Y., Matsuda, R., Uchida, T., Ikura, T. et al. (2009) The human actin-related protein hArp5: Nucleo-cytoplasmic shuttling and involvement in DNA repair. *Experimental Cell Research*, *315*, 206–217.

Klopf, E., Schmidt, H.A., Clauder-Munster, S., Steinmetz, L.M. & Schuller, C. (2017) INO80 represses osmostress induced gene expression by resetting promoter proximal nucleosomes. *Nucleic Acids Research*, *45*, 3752–3766.

Knoll, K.R., Eustermann, S., Niebauer, V., Oberbeckmann, E., Stoehr, G., Schall, K. et al. (2018) The nuclear actin-containing Arp8 module is a linker DNA sensor driving IN080 chromatin remodeling. *Nature Structural & Molecular Biology*, *25*, 823–832.

Kornberg, R.D. & Lorch, Y. (1999) Twenty-five years of the nucleosome, fundamental particle of the eukaryote chromosome. *Cell*, *98*, 285–294.

Lademann, C.A., Renkawitz, J., Pfander, B. & Jentsch, S. (2017) The INO80 complex removes H2A.Z to promote presynaptic filament formation during homologous recombination. *Cell Reports*, *19*, 1294–1303.

Lo, H.J., Kohler, J.R., DiDomenico, B., Loebenberg, D., Cacciapuoti, A. & Fink, G.R. (1997) Nonfilamentous *C. albicans* mutants are avirulent. *Cell*, *90*, 939–949.

Lu, Y., Su, C. & Liu, H.P. (2012) A GATA transcription factor recruits Hda1 in response to reduced Tor1 signaling to establish a hyphal chromatin state in *Candida albicans*. *PLoS Pathogens*, *8*, e1002663.

Luger, K., Mader, A.W., Richmond, R.K., Sargent, D.F. & Richmond, T.J. (1997) Crystal structure of the nucleosome core particle at 2.8 a resolution. *Nature*, *389*, 251–260.

Noble, S.M. & Johnson, A.D. (2005) Strains and strategies for large-scale gene deletion studies of the diploid human fungal pathogen *Candida albicans*. *Eukaryotic Cell*, *4*, 298–309.

Parker, J.C., Jr., McCloskey, J.J. & Knauer, K.A. (1976) Pathobiologic features of human candidiasis. A common deep mycosis of the brain, heart and kidney in the altered host. *American Journal of Clinical Pathology*, *65*, 991–1000.

Poli, J., Gasser, S.M. & Papamichos-Chronakis, M. (2017) The INO80 remodeller in transcription, replication and repair. *Philosophical Transactions of the Royal Society B: Biological Sciences*, *372*, 20160290.

Romani, L., Bistoni, F. & Puccetti, P. (2003) Adaptation of *Candida albicans* to the host environment: the role of morphogenesis in virulence and survival in mammalian hosts. *Current Opinion in Microbiology*, *6*, 338–343.

Shen, X.T., Mizuguchi, G., Hamiche, A. & Wu, C. (2000) A chromatin remodelling complex involved in transcription and DNA processing. *Nature*, *406*, 541–544.

Shen, X., Ranallo, R., Choi, E. & Wu, C. (2003) Involvement of actin-related proteins in ATP-dependent chromatin remodeling. *Molecular Cell*, *12*, 147–155.

Shimada, K., Oma, Y., Schleker, T., Kugou, K., Ohta, K., Harata, M. et al. (2008) Ino80 chromatin remodeling complex promotes recovery of stalled replication forks. *Current Biology*, *18*, 566–575.

Smith, C.L. & Peterson, C.L. (2005) ATP-dependent chromatin remodeling. *Current Topics in Developmental Biology*, *65*, 115-+.

Subramanian, V., Fields, P.A. & Boyer, L.A. (2015) H2A.Z: a molecular rheostat for transcriptional control. *F1000Prime Reports*, *7*, 01.

Sudbery, P.E. (2011) Growth of *Candida albicans* hyphae. *Nature Reviews Microbiology*, *9*, 737–748.

Szerlong, H., Hinata, K., Viswanathan, R., Erdjument-Bromage, H., Tempst, P. & Cairns, B.R. (2008) The HSA domain binds nuclear actin-related proteins to regulate chromatin-remodeling ATPases. *Nature Structural & Molecular Biology*, *15*, 469–476.

Takahashi, Y., Murakami, H., Akiyama, Y., Katoh, Y., Oma, Y., Nishijima, H. et al. (2017) Actin family proteins in the human INO80 chromatin remodeling complex exhibit functional roles in the induction of heme Oxygenase-1 with hemin. *Frontiers in Genetics*, *8*, 17.

Tosi, A., Haas, C., Herzog, F., Gilmozzi, A., Berninghausen, O., Ungewickell, C. et al. (2013) Structure and subunit topology of the INO80 chromatin remodeler and its nucleosome complex. *Cell*, *154*, 1207–1219.

Wang, L., Du, Y., Ward, J.M., Shimbo, T., Lackford, B., Zheng, X.F. et al. (2014) INO80 facilitates pluripotency gene activation in embryonic stem cell self-renewal, reprogramming, and blastocyst development. *Cell Stem Cell*, *14*, 575–591.

Wang, X., Zhu, W., Chang, P., Wu, H., Liu, H. & Chen, J. (2018) Merge and separation of NuA4 and SWR1 complexes control cell fate plasticity in *Candida albicans*. *Cell Discovery*, *4*, 45.

Whiteway, M. & Bachewich, C. (2007) Morphogenesis in *Candida albicans*. *Annual Review of Microbiology*, *61*, 529–553.

Willhoft, O. & Wigley, D.B. (2020) INO80 and SWR1 complexes: the non-identical twins of chromatin remodelling. *Current Opinion in Structural Biology*, *61*, 50–58.

Wyrick, J.J., Holstege, F.C.P., Jennings, E.G., Causton, H.C., Shore, D., Grunstein, M. et al. (1999) Chromosomal landscape of nucleosome-dependent gene expression and silencing in yeast. *Nature*, *402*, 418–421.

Yao, W., King, D.A., Beckwith, S.L., Gowans, G.J., Yen, K.Y., Zhou, C. et al. (2016) The INO80 complex requires the Arp5-Ies6 subcomplex for chromatin remodeling and metabolic regulation. *Molecular and Cellular Biology*, *36*, 979–991.

Zhang, X., Wang, X.J., Zhang, Z.H. & Cai, G. (2019) Structure and functional interactions of INO80 Actin/Arp module. *Journal of Molecular Cell Biology*, *11*, 345–355.

Zhao, S.M., Xu, W., Jiang, W.Q., Yu, W., Lin, Y., Zhang, T.F. et al. (2010) Regulation of cellular metabolism by protein lysine acetylation. *Science*, *327*, 1000–1004.

Zhu, W., Fan, X., Zhao, Q., Xu, Y., Wang, X. & Chen, J. (2021) Bre1 and Ubp8 regulate H2B mono-ubiquitination and the reversible yeast-hyphae transition in *Candida albicans*. *Molecular Microbiology*, *115*, 332–343.

SUPPORTING INFORMATION

Additional supporting information can be found online in the Supporting Information section at the end of this article.

How to cite this article: Zhao, Q., Dai, B., Wu, H., Zhu, W. & Chen, J. (2022). Ino80 is required for H2A.Z eviction from hypha-specific promoters and hyphal development of *Candida albicans*. *Molecular Microbiology*, *118*, 92–104. https://doi.org/10.1111/mmi.14954